

Tkachenko waves in rapidly rotating Bose-Einstein condensates

L. O. Baksmaty, S. J. Woo, S. Choi, N. P. Bigelow

Department of Physics and Astronomy, and Laboratory for Laser Energetics, University of Rochester, Rochester, NY 14627
(Dated: April 14, 2024)

We present a mean-field theoretical study of Tkachenko waves of a vortex lattice in trapped atomic Bose-Einstein condensates. Our results show remarkable qualitative and quantitative agreement with recent experiments at JILA. We extend our calculations beyond the conditions of the experiment, probing deeper into the incompressible regime where we find excellent agreement with analytical results. In addition, bulk excitations observed in the experiment are discussed.

PACS numbers: 03.75.Fi, 05.30.Jp, 42.50.Vk

The dynamics of quantized vortices are important in a wide variety of physical phenomena from turbulence to neutron stars, to superconductivity and superfluidity [1]. The broad relevance of this problem is partly responsible for the current interest in vortex lattices in trapped Bose-Einstein condensates (BECs). This system is also attractive because it can easily be manipulated and imaged [2, 3, 4] and because the condensate is accurately described within mean-field theory. Until recently much of the progress made in the study of vortex arrays in neutral superfluids was in the context of ^4He . This system however is notoriously difficult to manipulate and control. Vortex lattices in BECs have thus created an unprecedented opportunity to study vortex matter in detail. This has been recently demonstrated in spectacular experiments at JILA in which Tkachenko waves as well as hydrodynamic shape oscillations were directly observed [4]. In this paper we present a numerical study of these vortex matter excitations. Our approach has the advantage that it does not require any assumptions about the compressibility or homogeneity of the condensate.

In the limiting case of an incompressible irrotational fluid, Tkachenko waves are transverse vortex-displacement waves traveling in the triangular lattice of vortex lines which constitute the ground state of the rotating superfluid [5]. In this idealized situation, the size of the vortex core is infinitesimal and the dynamics of the fluid density may be ignored. For a simple illustration, consider a system of n vortices each of circulation k , in an irrotational, incompressible fluid of density ρ contained by a vessel rotating at angular frequency Ω . Let $\mathbf{v}(\mathbf{r})$ represent the fluid velocity at position \mathbf{r} . If the position of the i th vortex is labeled by a complex number z_i , the free energy (f) of the array may be written as

$$f = \frac{k^2}{4} \sum_{i=1}^n \sum_{j=1}^n \left(\frac{1}{2} \log |z_i - z_j|^2 + \frac{1}{2} \log |z_i|^2 + \frac{1}{2} \log |z_j|^2 \right) + \frac{1}{2} \sum_{i=1}^n \log |z_i|^2 \quad (1)$$

Here we ignore the effects of the boundaries and the energy associated with vortex cores [1, 8, 9]. By taking into account the irrotational ($\nabla \times \mathbf{v} = 0$) and incompressible ($\nabla \cdot \mathbf{v} = 0$) nature of the fluid, we may derive this expression from the simple classical relation for the energy

which in this case is purely kinetic:

$$f = \frac{1}{2} \int \rho(\mathbf{r}) \mathbf{v}(\mathbf{r})^2 d\mathbf{r} \quad (2)$$

We can observe from Eq. (1) that the vortex lattice, which represents a local minimum of this free energy, results from a competition between two terms: the logarithmic term which represents the intervortex repulsion, and the quadratic rotational term which pulls the vortices towards the center. The Tkachenko waves are organized as oscillations of the vortex positions about this equilibrium. On the microscopic level, the vortices precess about their equilibrium position in elliptical orbits against the trap rotation with the major axis perpendicular to the wave propagation. On the macroscopic scale, the array is seen to undergo harmonic distortions which shear the lattice and cause the rotation of the array to alternatively slow down and speed up.

Vortex arrays produced in rapidly rotating trapped BECs depart from this idealized case in two important aspects: the system is significantly compressible, and the underlying fluid is inhomogeneous. Due to finite compressibility, it is important to consider the dynamics of the underlying fluid for an accurate treatment. This is especially true in the light of recent interest in lattices in the mean-field quantum Hall regime [6, 7]. To date, most vortex lattice studies rely on incompressible hydrodynamic approximations [1, 8, 9, 10]. The hydrodynamic approximation restricts the calculation to long wavelength excitations and the assumption of incompressibility ignores the dynamics of the fluid density. Baym [11] has recently demonstrated the importance of compressibility to the description of current experimental data. The compressibility of the lattice may be gauged from the ratio ξ^2/λ^2 . Here ξ and λ are the healing length and intervortex distance respectively. The healing length estimates the size of the vortex core. We define these as $\xi = \sqrt{\hbar^2/mna}$ and $\lambda^2 = \hbar^2/2m\Omega$ [12], where a is the scattering length of the trapped species, n is the density at the center of the condensate and Ω is the angular frequency of the trap rotation. In this Letter we bypass these familiar approximations by adopting a full numerical approach based on mean-field theory.

As an initial step, we must construct the undisturbed vortex array to a high degree of accuracy. We focus on

the excitations of triangular vortex arrays with hexagonal symmetry, such as those obtained by recent experiments. A pancake shaped trap geometry is employed. We note that owing to the centrifugal reduction in the radial trap frequency ω_r , this is a reasonable assumption at high rotation frequencies where most of our studies take place. More importantly, the pancake geometry has been experimentally justified by the high quality of direct imaging of high [13] and low energy lattice excitations – if the curvature of vortex lines were significant, such imaging would not be possible. According to the $T = 0$ mean field theory, the condensate wavefunction in a frame rotating with angular velocity ω satisfies the equation

$$i\hbar \frac{\partial \psi(r;t)}{\partial t} = \left[\frac{\hbar^2}{2m} \nabla^2 + V(r) + N g \int |\psi|^2 L_z \right] \psi(r;t); \quad (3)$$

where m is the mass of the species, ω_r is the radial trapping frequency, N is the number of trapped atoms and L_z is the angular momentum operator defined as $i\hbar \frac{\partial}{\partial \phi}$. The coupling constant g and the external potential $V(r)$ are defined as $g = 4\hbar^2 a^2/m$ and $V(r) = \frac{1}{2}m\omega_r^2 r^2$ respectively. The corresponding stationary equation is solved using a steepest descent technique starting from a triangular seed array. We define the fluctuation of the order parameter by,

$$\psi = u(r)e^{i\omega t} + v(r)e^{i(\omega+1)t}; \quad (4)$$

Following the Bogoliubov-de Gennes procedure, first order expansion around the ground state in terms of ψ then yields the eigen-equation for the excitation amplitudes $u(r)$ and $v(r)$ [12]:

$$\begin{aligned} \left[\frac{\hbar^2}{2m} \nabla^2 + V(r) + 2N g \int |\psi|^2 L_z \right] u &= \epsilon u \\ \left[\frac{\hbar^2}{2m} \nabla^2 + V(r) + 2N g \int |\psi|^2 L_z \right] v &= -\epsilon v \end{aligned} \quad (5)$$

Unless otherwise stated, we express energy, length and time in the oscillator units $\hbar\omega_r$, $\sqrt{\hbar/m\omega_r}$ and $1/\omega_r$ respectively. For the solution of the coupled eigenvalue equation (Eq. (5)), we use a finite element method [14]. The eigenvalue problem is characterized by three length scales: the Thomas-Fermi radius $R_{TF} = \sqrt{2}/\omega_r$, the healing length ξ , and the inter-vortex spacing λ . R_{TF} specifies the extent of the lattice, and ξ and λ constrain the density of the grid required by the calculation. Care must be taken to ensure the grid captures features over these length scales and this renders the problem very computationally expensive. It was not unusual to obtain sparse matrices of the order $10^5 \times 10^5$; to solve such large eigen-systems, we used a variety of numerical libraries and visualization tools [15].

Following Ref. [10], we represent a Tkachenko wave by a complex valued function $D_{n,m}(r;t)$ defined by

$$D_{n,m}(r;t) = e^{i[f_{n,m}^a(r) \sin(m\omega_r t) + f_{n,m}^b(r) \cos(m\omega_r t)]} \quad (6)$$

The integer pair (n,m) represent the radial and angular order of the excitations, $r = (r; \phi)$, is an arbitrary phase and $f(f_{n,m}^a(r); f_{n,m}^b(r))$ are real valued functions. The real and imaginary part of $D_{n,m}$, represent the displacement of a vortex at r along the x and y axis respectively. According to $D_{n,m}$, every vortex moves in an elliptical path.

One of the challenges of comparing our numerical calculation to experiment or to analytic results is the proper identification of the excitations obtained. In our calculation, the degree of freedom is the fluctuation of the field

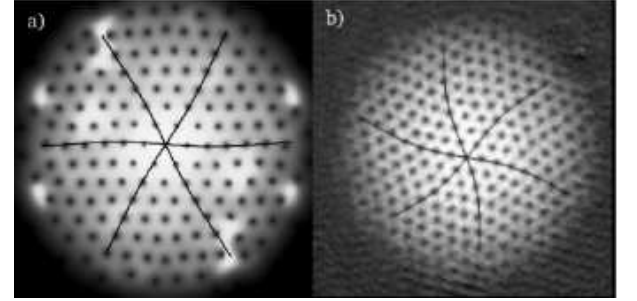


FIG. 1: Both figures depict a snapshot of the $(1,0)$ mode in action. a) Simulation. b) Result from the JILA experiment. The curve is a fitted sine wave of wavelength $1.33R_{TF}$

amplitude $\delta\psi$, while in analytical work it is the distortion $D_{n,m}$ of the vortex array that is employed. One approach, involves making "movies" of each excitation by using Eq. (4). In Figs. 1 and 2, we show snapshots from two such movies for the $(1;0)$ and $(2;0)$ modes and compare them to experimental data. This technique however, has limitations. Even with a high-resolution movie, the excitations are usually difficult to tell apart by eye, especially as ω_r^2 grows. The largely transverse Tkachenko waves become increasingly corrupted by sound waves traveling in the underlying fluid which scatter off the vortices. A more rigorous and reliable approach involves extracting the distortion $D_{n,m}$ from the fluctuation induced by a particular excitation.

We therefore adopted a quantitative approach based upon determining the instantaneous position of each vor-

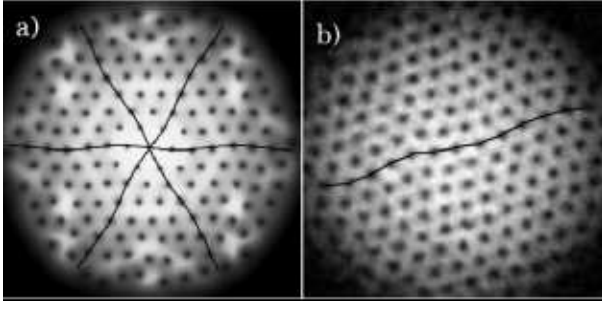


FIG. 2: (2,0) m mode in action. a) Simulation. b) Result from the JILA experiment. In both cases, the curves are drawn to guide the eye.

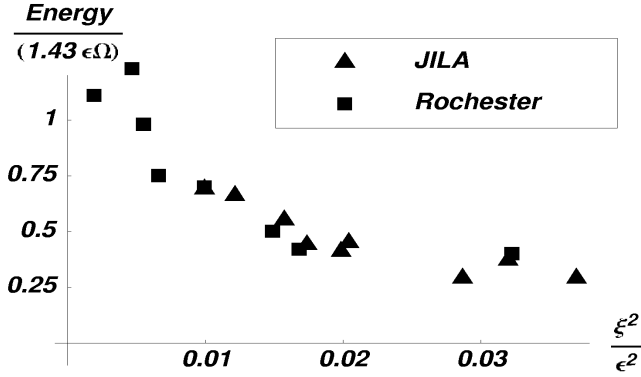


FIG. 3: Energy of the (1,0) m mode vs. ξ^2/ϵ^2 . In Ref. [10] the energy of this mode is given as 1.43.

tex. A coarse distortion function $D_{n,m}$ can then be constructed by interpolating on the triangular lattice which specifies the groundstate. Along any circle centered at the origin, r is constant and the interpolated distortion $D_{n,m}$ defines a one dimensional function $d(\phi)$. The Fourier transform of $e^{i\phi} d(\phi)$ then yields a peak near

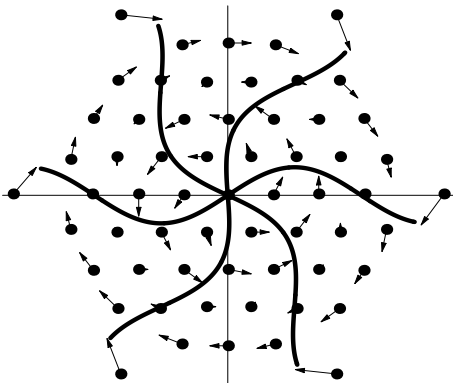


FIG. 4: Distortion of an array $\xi^2/\epsilon^2 = 0.007$ in a (1,0) m mode. The dots represent the equilibrium positions of the vortices, and the straight arrows represent the actual calculated vortex displacements. The curve is a fit of a sine wave of wavelength $1.33R_{TF}$ to the vortex displacements.

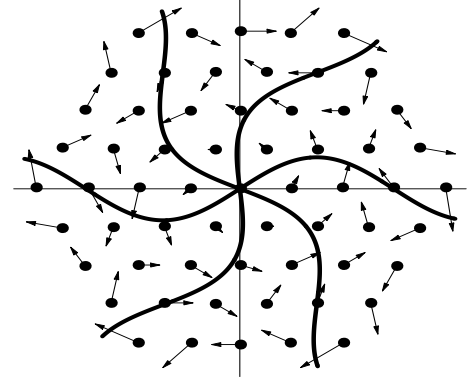


FIG. 5: Distortion of an array $\xi^2/\epsilon^2 = 0.032$ in a (1,0) m mode. Compare with Fig. 4, where ξ^2/ϵ^2 is much smaller. All symbols have the same meaning as in Fig. 4.

the value m for the excitation labeled by $(n;m)$. This analysis reveals one important result: the sense of precession of each vortex in an $m \neq 0$ mode may either be with or against the trap rotation. In these modes the sense of precession of a vortex is a function of its radial coordinate only, and along any circle all vortices precess in the same sense. This is a dramatic departure from the ideal situation of an array in a uniform, irrotational and incompressible uid. In that case the vortices precess only against the trap rotation. We note that this has been analytically examined [16].

Our central result is illustrated by Fig. 3, where we make a quantitative comparison with the JILA experiment [4] and with recent analytic results [10]. We focus on the (1;0) m mode. As the parameter ξ^2/ϵ^2 is lowered (abscissa), we observe a quantitative deviation from analytic results (unity line on the ordinate) which is indistinguishable from that experimentally reported [4]. In proportion to this deviation, we find that the eccentricity of the elliptically polarized vortex oscillations in the Tkachenko wave is reduced and the individual vortex motion become almost circular. We illustrate this trend in Figs. 4 and 5 (to be compared with Fig. 3 (b) in Ref. [10]). Notice that the vortex displacement vectors in Fig. 5 have a more significant longitudinal projection than in Fig. 4 in which the ratio ξ^2/ϵ^2 is almost an order of magnitude larger. In the opposite limit as $\xi^2/\epsilon^2 \rightarrow 0$, we obtain very good agreement with the analytical results. We point out that it is not surprising that our energies begin to exceed the analytic value (unity line). In the analytic treatment [10], the energy of this mode was calculated to first order in ξ^2/ϵ^2 . For small ξ^2/ϵ^2 , we consider arrays for which $\xi^2/\epsilon^2 \leq 0.2$ and for which higher order terms in ξ^2/ϵ^2 could be important.

In the limit of an incompressible uid, the potential energy of the system is quenched and Tkachenko waves emerge as the only nontrivial class of excitations of a vortex array. However, they are just one of several types of excitations which may occur within the compressible vortex arrays realized in experiments [1]. Of particular are

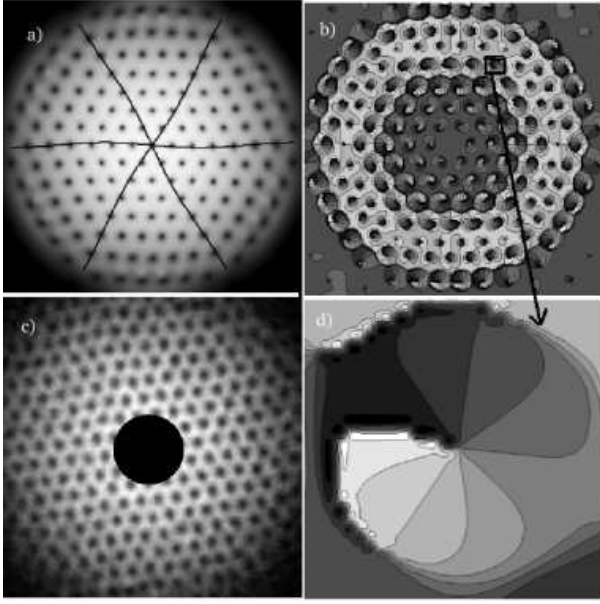


FIG. 6: a) A bulk (2,0) mode in action. The curve is a sine wave of wavelength $1.33R_{TF}$ predicted for the (1,0) Tkachenko wave. b) Phase plot of Eq. (7). Notice the phase change as you radially cross a node. c) Approximate region in the array from which atoms are removed to excite the (2,0) bulk or (1,0) Tkachenko modes in the JILA experiment. d) Close-up of b) on the location of a vortex. In both of the phase plots above, phase changes from 0 to 2 as you go from dark to light regions.

the bulk modes [17, 18, 19], some of which can be very similar in appearance to Tkachenko waves. In Ref. [4], the observation of a rapid mode which is visually indistinguishable from the Tkachenko (1,0) mode is reported. We also identify such a mode at exactly the experimentally reported value of $2.25! -$ this is just the second order bulk breathing or (2;0) mode viewed in a rotating frame.

During each half of the linear oscillatory motion imposed on the vortices by the breathing action, the transverse (Magnus) force acts in opposite directions. On a microscopic level, elliptical motion of the vortices is observed. Macroscopically, the array twists around the center of rotation like a torsional pendulum as the density breaths radially. We depict this second order 'breathing' mode in Fig. 6 a). Surprisingly, the sine wave radial distortion predicted [10] for the (1;0) Tkachenko mode is also in very good agreement with this (2;0) bulk mode. To further illustrate this point, we make use of the complex density fluctuation defined for the n th excitation by [17],

$$= (u_n \quad v_n): \quad (7)$$

A casual comparison of the phase of for this mode in Fig. 6 b) with a schematic of the experimental probe in Fig. 6 c) confirms the correct identification of the mode excited in the experiment. A close up of this phase plot around the position of a vortex is shown in Fig. 6 d). This describes a clockwise elliptical oscillation of the density fluctuation which has a local peak at the vortex core. A similar motion of the vortex at this site is implicated. We predict the existence of third and fourth order breathing modes at $2.55!$ and $3.30!$ respectively. This is a clear example of how the presence of a transverse force may blur the visual distinction of the largely longitudinal modes from the transverse Tkachenko waves [1]. We have observed promising candidates for the differential longitudinal waves which have been suggested previously [4]. In these relatively high energy excitations, vortex oscillations drive and are driven by large scale fluid density fluctuations. We shall report on these modes elsewhere.

We thank Michael Banks for valuable computing assistance and G. S. Krishnaswami for insightful discussions. We are also grateful to E. A. Comell for permission to present the JILA data. L. O. Bakshi is a Horton Fellow. This work is supported by NSF, ARO and ONR.

-
- [1] E. B. Sonin, Rev. Mod. Phys. 59, 87 (1987).
 - [2] C. Raman et al., Phys. Rev. Lett. 87, 210402 (2001); J. R. Abo-Shaer et al., Phys. Rev. Lett. 88, 070409 (2002).
 - [3] P. C. Haljan et al., Phys. Rev. Lett. 87, 210403 (2001).
 - [4] I. Coddington et al., e-print cond-mat/0305008.
 - [5] V. K. Tkachenko, Soviet Physics JETP 23, 1049 (1966).
 - [6] Tin-Lun Ho, Phys. Rev. Lett. 87, 060403 (2001).
 - [7] E. A. Comell, Personal communication.
 - [8] L. J. Campbell and R. M. Zi, Phys. Rev. B 20, 1886 (1979).
 - [9] L. J. Campbell, Phys. Rev. A 24, 514 (1981).
 - [10] J. Anglin and M. Cressinanno, e-print cond-mat/0210063.
 - [11] G. Baym, e-print cond-mat/0305294.
 - [12] A. L. Fetter and A. A. Svidzinsky, J. Phys. Condens. Matter 13, R135 (2001).
 - [13] P. Engels et al., Phys. Rev. Lett. 89, 100403 (2002).
 - [14] See, Strang and Fix, An analysis of the finite element method, Strang and Fix (Prentice-Hall, Inc., Englewood Cliffs, N.J. 1973).
 - [15] PARPACK (www.caam.ripc.edu/software/ARPACK); PETSC (www-unix.mcs.anl.gov/petsc/petsc-2/); Numerical recipes in FORTRAN 90 (Cambridge University Press, 1996); PVWAVE; IMSL (www.vni.com).
 - [16] J. Anglin and M. Cressinanno, Personal communication.
 - [17] A. A. Svidzinsky and A. L. Fetter, Phys. Rev. A 58, 3168 (1998).
 - [18] S. Choi, L. O. Baksmaty, S. J. Woo and N. P. Bigelow, e-print cond-mat/0306549.
 - [19] M. Cozzini and S. Stringari, Phys. Rev. A 67, 041602(R) (2003).